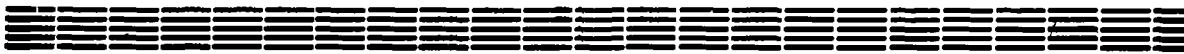


Preprint YERPHI-1305(91)-90

(Efi--1305-91-90).

ԵՐԵՎԱՆԻ ՖԻԶԻԿԱԶԻ ԻՆՍՏԻՏՈՒՏ
ЕРЕВАНСКИЙ ФИЗИЧЕСКИЙ ИНСТИТУТ
YEREVAN PHYSICS INSTITUTE



R.G. BADALYAN

FAST HADRON FORMATION MECHANISM
IN LEPTOPRODUCTION ^{Processes} IN NUCLEI

ЦНИИатоминформ
ЕРЕВАН-1990

Ռ.Գ.ԲԱԴԱԼՅԱՆ

ԱՐԱԳ ՀԱԴԻՐՈՆՆԵՐԻ ՁԵՎԱՎՈՐՄԱՆ ՄԵԽԱՆԻԶՄԸ ՄԻՋՈՒԿՆԵՐԻ
ՄԵՋ՝ ԼԵՓՔՈՇՆՄԱՆ ԳՐՈՑԵՍՈՒՄ

Քննարկված են խորը ոչ-առածգական տիրույթում արագ հաղորդների լեփթոծնման տարբեր մեխանիզմներ ատոմային միջուկներում; Վերլուծված են վիրտուալ ֆոտոնի հատվածավորման տիրույթում արագ հաղորդների ձեւավորման պրոցեսի տարբեր հնարավոր մեխանիզմները և միջուկային նյութով քվարկի (քվարկ-գլյուոնային համակարգի) շարժման պրոցեսը: Տույց է տրված, որ $19\text{ էվ}^2 \leq Q^2 \leq 49\text{ էվ}^2$ և $59\text{ էվ} \leq \nu \leq 109\text{ էվ}$ կինեմատիկական տիրույթը համեմատաբար բարենպաստ է՝ վիրտուալ ֆոտոնից ծնված քվարկի (քվարկ-գլյուոնային համակարգի) լայնակի չափերի աճի (Էվոլյուցիայի) օրենքի ուսումնասիրման համար: Ուսումնասիրված է հաղորդների լեփթոծնման նկատմամբ միջուկների թափանցիկության կախվածությունը հաղորդաչան տարածա-ժամանակային բնութագրերից τ և σ_q , ինչպես նաև վիրտուալ ֆոտոնի կինեմատիկ բնութագրերից Q^2 , ν և գրանցվող հաղորդի E_h էներգիայից:

Երևանի ֆիզիկայի ինստիտուտ

Երևան 1990



Introduction

The process of lepton production on nuclei in deep inelastic region, from the point of view of the physics of strong interactions contains an interesting information on the process of leading hadron formation from constituents (quarks and gluons) as well as on propagation of quarks and quark-gluon systems in nuclear matter [1-9].

Many works are devoted to the investigation of the mechanism of hadron formation from quarks and gluons in the region of fragmentation of different quark-gluon systems (QGS hadronization) in the frameworks of different phenomenological models [10-14]. All these works can be divided into several main groups. To the first group can be related the works where on the basis of integral equations for fragmentation functions the iterational (cascade) model is developed [15-18], the mechanism of hadronization being, in general, out of the frameworks of this approach. To the next group can be related the works [19,20] in which the parameters of fragmentation functions of "dressed" quarks are connected with the characteristics of the corresponding Regge trajectories. In particular, in [20] in the frameworks of the quark-gluon string model the expressions for the fragmentation functions for "dressed" quarks and diquarks were obtained in the regions $x \rightarrow 0$ and $x \rightarrow 1$, and a method was proposed for reconstruction of these functions by their utmost behaviour.

The process of fragmentation of quarks and gluons on the

basis of QCD cascade is considered in [21,22] where the hadronization process is reduced to the production of colourless massive formations by their successive decay into observable hadrons. To the fourth group one can relate the LUND string fragmentation model [23], in which the hadronization mechanism has a kinematical nature (the quark and antiquark produce a meson, if the mass of the quark-antiquark pair is less than some characteristic mass). And, at last, there is the fifth group of models [24-30], where assumptions on the recombination nature of the hadron formation in the fragmentation region [31-34] (which corresponds to short-range interaction in the space of rapidities [33]) are made.

The present work is devoted to consideration of the quark (quark-gluon system) propagation in nuclear matter, though it seems probable that the processes of the fast hadron formation and propagation of quarks in nuclear matter can occur simultaneously and influence on each other and be caused by each other. However, in the present work, as in [1-8], it is supposed that the nucleus plays a passive role in the process of fast hadron formation or, in other words, the presence of nucleus just allows to register the changes in the character of the quark (quark-gluon system) and nucleon interactions or the time evolution of quark-gluon system, but it has no influence on the hadron formation. It should be noted, that the role of the nucleus in the hadronization process in the frameworks of the LUND model is considered in Ref.[9] from another point of view.

At present there is no clear understanding of the mechanism of the leading hadron formation from quarks and gluons as well as of propagation of quarks in nuclear matter. The main difficulty here is the presence of truly strong interactions (non-perturbative QCD effects) in the final stage of hadron

formation from quarks and gluons. However, in the presence of a hard subprocess with $Q^2 \gg m_c^2$, where m_c is some characteristic mass, the value of which will be obtained later, the time that characterizes the hard subprocess $\tau_p \approx \omega/Q^2$ is less than the time of transformation of the quark (quark-gluon system) produced in this subprocess, into normal hadron at $\tau_F \approx \omega/m_c^2$. This fact, apparently, will allow one to consider the hadron formation process on the level of quasiclassical description in the frameworks of probabilistic representations, because the interference between the regions $t \sim \tau_p$ and $t \sim \tau_F$ will be suppressed at $\tau_F \gg \tau_p$.

Let us consider in details the mechanism of interaction of virtual photon having four momentum $q^\mu = (\nu, 0, 0, \xi)$ and $q^\mu q_\mu = -Q^2 < 0$ with a nucleus in rest. The lifetime of such a photon, in contrast to the real photons, is limited by $\tau_{\gamma^V} \approx 2\nu/Q^2$ [35-38]. In the rest system of nucleus the photon is transformed into a quark-antiquark pair, and this pair in order to interact with the nucleons of nucleus during a time less than or of the order of τ_{γ^V} , has to be asymmetric by momentum, because in a symmetric pair both quark and antiquark have a large momentum of $\sim \nu/2$, and during a time of the order of τ_{γ^V} they will not manage to regenerate their long wave gluonic field, or in the language of the parton model, during the time τ_{γ^V} the parton stair of quark and antiquark do not manage to develop up to the wee-parton [35,36] and quark-antiquark (hadronic or quark-gluonic) fluctuation of photon collapses, having no time to be potent for a strong interaction.

In case of an asymmetric pair the slow antiquark (quark) manages to regenerate the long-wave component of its gluonic field during the time interval $\tau_p \approx \omega/Q^2$ and annihilates with the

quark (antiquark) of nucleons in nucleus. The degree of asymmetry is determined by the condition that the slow antiquark (quark) of the pair during the lifetime of virtual photon τ_{γ^v} has to have time enough for regeneration of the long-wave component of its gluonic field (quark-gluon sea) and it is equal to $p_S^{\parallel}/p_F^{\parallel} \approx m_c^2/Q^2$, where p_S^{\parallel} and p_F^{\parallel} are the longitudinal momenta (with respect to the direction of virtual photon momentum) of the slow and fast components of the quark-antiquark pair, respectively. So, during the time interval $\tau_p \approx \omega/Q^2$ the slow antiquark (quark) of the pair gets time to develop its parton stair up to wee-partons, i.e. it is transformed into an additive or constituent antiquark (quark) or a valon, and annihilates with the quark (antiquark) of the nucleons in nucleus. Such a picture, obviously, is not a Lorentz-invariant one, and the annihilation mechanism cannot be an arbitrary one, but it has to have such a structure, that during transition to other frames, say, to the Breit frame, it has to provide the standard picture of the quark "knock out" from the nucleon of nucleus. For that, the participation of the spectator quarks of the nucleon in the process of annihilation of the antiquark from the pair seems necessary (see Fig. 1).

After annihilation of the slow antiquark (quark), the fast quark (antiquark) of the pair continues its movement, but the cross section of its interaction with nucleons in nucleus is remarkably less (in proportion with Q^2/m_c^2 [4.5]) than that of the normal hadron due to the fact, that in the gluon field (quark-gluon field) of such a "semidressed" quark the long-wave component is absent, which has no time to regenerate in the time interval τ_p , and which appears only in a time interval of the order of τ_F .

There exist different conceptions of the colour and compo-

sition of the quark-gluon system or the parton jet that produces the fast quark of the pair in the process of evolution. In Refs. [39,40] a mechanism is offered, which makes the quark-gluon jet colourless at the time interval of $\sim\tau_p$, i.e. to the moment of annihilation of the slow antiquark of the pair.

In the frameworks of such a picture the quark-gluon system looks like a white quark-antiquark string having a fast quark and a slow antiquark on its ends. Such a string starts its hadronization in time intervals of the order of τ_p , when the end slow antiquark hadronizes and the wave of hadronization reaches the fast quark at the moment $\sim\tau_F$, when a leading hadron containing a fast quark is formed [39,40].

Another scenario of fast hadron formation is developed in [4], where it is supposed that the leading hadron, which contains a fast quark, is formed during a time interval of the order of τ_p , but its transverse dimensions are m_c^2/Q^2 times smaller than the hadron size. Such a compressed colour dipole transforms into a normal hadron in a time interval of $\sim\tau_F$ and only then its cross section of interaction with the nucleons in nucleus becomes equal to the hadronic cross section σ_h .

Thus, in the described pictures of the fast hadron formation the general point is the fact, that during a time interval of $\sim\tau_p$ a quark-gluon system (quark or quark-antiquark string or colour dipole) is formed in/from which in τ_F time a fast hadron is formed that contains a leading (valence) quark of this system. The cross section of interaction of such a system starts increasing from the value $\sigma_q \approx (m_c^2/Q^2)\sigma_h$ at the moment τ_p up to the value σ_h at the moment of the leading hadron formation.

This law of the cross section change from σ_q to σ_h cannot be predicted in the frameworks of perturbative QCD, at least in

the region $t < \tau_F$, where t is time or space variable. At sufficiently high values of $Q^2 \gg m_c^2$ for the region $t \geq \tau_p$ in the frameworks of perturbative QCD one can get predictions for $\alpha(t) \sim t$ [1,2,5,8] the so-called model of quantum diffusion at which the transverse dimension of quark-gluon system increases as \sqrt{t} , because the points of the appearance of quark-antiquark pairs or gluons in the transverse plane are situated on the trajectory of Brownian particle [5,36,37]. On the other hand, in the frameworks of the colour dipole model one can expect $\alpha(t) \sim t^2$ [4,5].

The predictions for the value $R = \sigma(\gamma^V A + hX) / A\sigma(\gamma^V N + hX)$ depending on the type of the function $\alpha(t)$ will be discussed in the next section of the present work.

The picture of hadron formation discussed above supposes, apparently, the necessity of the condition $\alpha(\gamma^V A) \gg A\alpha(\gamma^V N)$ for the total cross section of absorption of the virtual photon by the nucleus and nucleon, respectively, i.e. the absence of the effects connected with the screening of just the photon interaction with the nuclear matter. The experimental data on deep inelastic interactions of leptons with nuclei [41-43] show that the effects connected with the screening of $\gamma^V A$ interaction are characterized by the variable $x_B = Q^2 / 2m_N \nu$ and in the region $0.05 \leq x_B \leq 0.3$ we have $\alpha(\gamma^V A) \gg A\alpha(\gamma^V N)$. In the present work a region of Q^2 and ν variables is considered, where the effects connected with the $\gamma^V A$ -interaction screening are absent, i.e. the region of $0.05 \leq x_B \leq 0.3$.

At present, very few experiments on studying the inclusive production of hadrons in the interactions of leptons with atomic nuclei are carried out. In Ref. [44] for the first time the increase of the transparency (decrease of absorptive power) to the yield of fast charged products of the virtual photon

hadronization from nucleus was observed. However, these data fail to provide getting a sufficiently detailed information on the parameters that characterize the space-time picture of the process of hadron formation. This is on the one hand due to the low statistical accuracy, on the other hand, due to averaging of the data in remarkably wide intervals of ν (from 3GeV to 17GeV at $\bar{\nu}=10\text{GeV}$) and Q^2 (from $Q^2=0.35\text{GeV}^2$ to 1GeV^2 , and from $Q^2=1\text{GeV}^2$ to 5GeV^2).

In another experiment, [45], conducted by EMC at CERN on muon beams with $E_\mu=200\text{GeV}$, there were also detected charged hadrons in the virtual photon fragmentation region. At $\nu \geq 100\text{GeV}$ and higher, a nearly full transparency of nuclear matter to the leptonproduction of hadrons was observed. The analysis of these experiments as well as the antineutrino experiment at energies of antineutrino $E_\nu < 30\text{GeV}$ does not allow one to get more or less definite information about the characteristic scales of the quark hadronization process. Thus, e.g. the estimates of the parameter m_C^2 obtained in [46] and [45] are $(0.08 \pm 0.04)\text{GeV}^2$ and $\sim 2\text{GeV}^2$, respectively. Let us however mention, that the data obtained in [45] at large values of $z \sim 0.7$ have a low statistical accuracy.

In section 2 of this work, on the basis of the analysis of the experimental data available now, it is shown that it is possible to give a self-consistent description of the experimental data of SLAC [44] and EMC CERN [45], if the value of m_C^2 is within the range $0.2\text{GeV}^2 \leq m_C^2 \leq 0.3\text{GeV}^2$ in case of the model $\alpha(t) \sim t$ and $0.3\text{GeV}^2 \leq m_C^2 \leq 0.5\text{GeV}^2$ in case of the model $\alpha(t) \sim t^2$. So, to get information definite enough on the parameters which characterize the space-time structure of the hadron formation mechanism, both experimental and theoretical investigations in this direction are important from the viewpoint of the dynamics

of strong interactions.

It is necessary to note, that within the next few years such experimental investigations will be carried out at the Yerevan electron synchrotron [47] as well as in SLAC in the frameworks of the PEGASYS/MARK II collaboration [48].

1. Nuclear Matter Transparency and its Dependence on Hadronization Characteristics

As a characteristic of the space-time structure of hadron leptoproduction, it is convenient to use the transparency of nuclear matter, which is defined as the ratio of the differential cross section of hadron leptoproduction on nucleus normalized to atomic weight to that on nucleon: $R = \sigma(\gamma^V A \rightarrow hX) / A \sigma(\gamma^V N \rightarrow hX)$. Nuclear transparency is minimal when the hadron is produced directly at the interaction point of an incident particle with nucleus and the produced hadron h is able then to interact inelastically with intranuclear nucleons with the cross section σ_h coinciding with the usual cross section of hN -interaction [38], the hadron propagation in nuclei being possible to be described in the conventional Glauber model [49]. The value of transparency is equal to the probability for the hadron to leave the nucleus without any inelastic interactions within it, i.e. without losing some notable portion of its primary energy. It is worth while to add in this connection, that in further calculations and comparison of nuclear transparency in leptoproduction process with experimental data available, one should restrict himself to considering the high-energy part of the inclusive spectrum of hadron (i.e. to large values of the variable $z = E_h / \nu$, where E_h is the energy of

detected hadron), as the contribution of secondary inelastic processes in nuclear matter to this range of the spectrum is insignificant.

Within relatively higher values of the variable $z \geq (0.5-0.7)$ the dominant contribution of inclusive hadron spectra is their direct production, that is, of the hadrons produced in the interaction process or in the formation process in the stage of leading quark evolution, but not of the hadrons produced from higher hadronic resonance decays. As it is shown in Refs. [30,50], in the fragmentation region of different quark-gluon systems, the contributions from decays of mesonic resonances in the inclusive spectrum of π -mesons are less than or equal to (10-20)% in the range of $z \geq (0.5-0.7)$. This is the reason why the region of relatively higher value of z is preferable, as the information on the mechanism of photon-nucleon interaction as well as on the propagation of quarks and/or hadrons through nuclear matter carry the direct hadrons.

If the leptoproduction process occupies a finite space-time interval, then the transparency is higher than the minimum value which is the limit of the Glauber scheme [49]. The maximum value equal to unity is achieved when the hadron is formed outside the nucleus and its constituents may interact in the nucleus with negligible cross section. If the mean absorption path of virtual photon in nuclear matter much exceeds the size of nucleus (which is the case for not so small values of the Bjorken variable $x_B > 0.05$ [38]), then the probability that the fast quark produced at the instant τ_p and the fast hadron induced by it in τ_f time will not undergo inelastic interactions in the nucleus, is determined by the expression [1-5,49]:

$$R = 1/A \int \rho(b,x) \exp\left(- \int_x^\infty \rho(b,t) \sigma(t) dt\right) dx d^2b \quad (1)$$

where $\rho(b, x) = \rho(r) = \rho_0 / (1 + \exp((r - r_A)/a))$ is the nuclear distribution density normalized to the condition $\int \rho(r) d^3r = A$, $b = |\vec{b}|$, $r = \sqrt{b^2 + x^2}$; $a = 0.54$ and $r_A = (0.978 + 0.0206A^{1/3})A^{1/3}$ [2], $\sigma(t)$ is the cross section of interaction of the quark into which the virtual photon is transformed on the point $\vec{r} = (\vec{b}, x)$, with the intra-nuclear nucleons. This cross section changes from σ_q in the point $t = x$ to σ_h at $t \gg (x + \tau)$, where τ is the characteristic time of the quark transition to hadron ($\tau \approx \tau_F$).

The dependence of the value of nuclear transparency R on A , τ , and σ_q , is given at different values of the two others in Figs. 2-5, respectively, assuming that $\sigma_h = 20 \text{ mb}$, which is the characteristic value of the meson-nucleon cross section.

The results of calculations for two models are shown. The first is based on perturbative QCD (the so-called quantum diffusion model), in the frameworks of which $\sigma(t) \approx \sigma_q + (\sigma_h - \sigma_q)t/\tau$ for $t/\tau \ll 1$, and the second one is based on a model, in the frameworks of which the quark-antiquark pair produced in the initial stage of interaction, i.e. the time τ_p is presented in the form of a coloured dipole that interacts with cross section $\sigma(t) \approx \sigma_q + (\sigma_h - \sigma_q)(t/\tau)^2$ at $t/\tau \ll 1$. The behaviour of $\sigma(t)$ near $t/\tau \approx 1$ refers to the non-perturbative QCD and cannot be given in the frameworks of perturbative QCD. Note, however, that the form of this function in the range $t/\tau \approx 1$ does not essentially influence the value R , which is mainly determined by the behaviour of $\sigma(t)$ function in the range $t/\tau \ll 1$.

The expressions for $\sigma(t)$ functions used to obtain numerical results in the frameworks of different models, are given in the Appendix.

It follows from the results presented in Figs. 2-5, that the difference between the behaviour of $\sigma(t) \sim t$ and $\sigma(t) \sim t^2$ is expected to be small and poorly observable both for small $\tau \lesssim F$

and large $\tau \geq 30F$. The ranges optimal for studying the dependence of the behaviour of the cross section $\sigma(t)$ on the time scale t are $3F \leq \tau \leq 30F$, and $\sigma_q \leq 10\text{mb}$.

2. Dependence of Nuclear Transparency on the Variables of Virtual Photon and Fast Hadron

The dependence of τ and σ_q on the kinematical variables of virtual photon, Q^2 and ν , and of the fast hadron registered, $z = E_h/\nu$, has been discussed by different authors [1-9]. In accordance with the modern concepts based on perturbative QCD, for these dependence one can expect [2,4,5]:

$$\tau = z\nu/m_c^2 \quad (2)$$

$$\sigma_q = (m_c^2/Q^2)\sigma_h \quad (3)$$

where m_c is some characteristic mass, the value of which can be defined from the experimental data available.

As noted, the experimental data available now are not self-consistent and not able to define the value of the parameter m_c^2 with sufficiently high accuracy. The results of our analysis carried out on the basis of the expressions (1)-(3) in the frameworks of the quantum diffusion model $\sigma(t) \sim t$, are presented in Figs.6-7. The SLAC data [44] are described satisfactorily when $m_c^2 = (0.22-0.48)\text{GeV}^2$, while to describe the EMC CERN data [45], it is necessary to have the value of $m_c^2 = (0.1-0.31)\text{GeV}^2$ (see Fig.8). Hence, it follows from the experimental data available, that the value of m_c^2 is within $0.2\text{GeV}^2 \leq m_c^2 \leq 0.3\text{GeV}^2$.

In the frameworks of the colour dipole model $\sigma(t) \sim t^2$, the agreement of the SLAC and EMC CERN data is better, but the

"range of consistency" over the variable m_C^2 is shifted towards higher values of m_C^2 , $0.3\text{GeV}^2 \leq m_C^2 \leq 0.5\text{GeV}^2$ (see Fig.8).

So, estimation of the value of m_C^2 allows us to find the kinematical region of Q^2 and ν favourable for investigation of the behaviour of the cross section $\sigma(t)$ vs. the time variable t . Fig.9 shows the nuclear transparency for ^{64}Cu nuclei to π -meson leptonproduction as a function of m_C^2 and m_C^2/Q^2 . As follows from Fig.9a, high sensitivity of R to the value of m_C^2/Q^2 occurs when $m_C^2/Q^2 \leq 0.5$, and the difference between the models $\sigma(t) \sim t$ and $\sigma(t) \sim t^2$ is maximal within $0.05 \leq x_B \leq 0.3$ and $0.05 \leq m_C^2/Q^2 \leq 0.5$. With account of the estimate of the variable m_C^2 , $0.2\text{GeV}^2 \leq m_C^2 \leq 0.5\text{GeV}^2$, one can find the favourable range for the virtual photon variables, $1\text{GeV}^2 \leq Q^2 \leq 4\text{GeV}^2$ and $6\text{GeV} \leq \nu \leq 10\text{GeV}$, to determine the behaviour of the cross section $\sigma(t)$ vs. the time variable t .

As it follows from Fig.10, for $Q^2/m_C^2 \geq (10-20)$ the value of nuclear transparency R is practically independent of the value of Q^2/m_C^2 , while for $Q^2/m_C^2 < 10$ the expected dependence of R on Q^2/m_C^2 is experimentally observable. On the other hand, the range of $Q^2/m_C^2 < 10$ is also interesting for the fact, that in this range there takes place a transition from the Glauber value for the nuclear transparency to the characteristic maximum value for R at the given photon energy ν . However, within the range $Q^2/m_C^2 < 10$ the non-perturbative QCD effects may be of importance (power corrections, such as higher twist and such things [51,52], which at $Q^2/m_C^2 = 10$, may reach ~10% and increase with decreasing Q^2), and about which it is hard to do any theoretical predictions, that is why the experimental investigation of the dependence of R on Q^2 in this range is of particular interest.

Conclusion

The main results obtained in this work are formulated as follows:

- The possibility of experimental investigation of the law of a quark's (a quark-gluon system's) evolution into a hadron depending on the time/space variable is shown;

- The favourable range for investigation of the behaviour of the cross section $\sigma(t)$ vs. t , i.e. $3F \leq t \leq 30F$ and $\sigma_q \leq 10\text{mb}$ in case of fragmentation to meson, is determined;

- It is shown, that when $Q^2/m_c^2 \geq (10-20)$, the nuclear transparency R is practically independent of the value of τ - the quark hadronization time;

- For the "range of consistency" of the SLAC [44] and EMC CERN data [45] it is obtained $0.2\text{GeV}^2 \leq m_c^2 \leq 0.3\text{GeV}^2$ for the model $\sigma(t) \sim t$, and $0.3\text{GeV}^2 \leq m_c^2 \leq 0.5\text{GeV}^2$ for the model $\sigma(t) \sim t^2$;

- It is shown that by the virtual photon variables Q^2 and ν in the ranges $1\text{GeV}^2 \leq Q^2 \leq 4\text{GeV}^2$ and $6\text{GeV} \leq \nu \leq 10\text{GeV}$ the difference between the models $\sigma(t) \sim t$ and $\sigma(t) \sim t^2$ is maximal.

Thus, it follows from the results presented in this work, that the hypothesis about a passive role of the nucleus in the fast hadron formation process is not to be ignored yet.

In conclusion the author would like to express his gratitude to A.Ts.Amatuni, H.H.Vartapetyan and S.H.Matinyan for support and collaboration, to K.A. van Bibber for interest and helpful discussions, and to A.O.Gasparyan, H.R.Gulkanyan and H.G.Mkrtchyan for discussions of the results obtained in this work.

APPENDIX

Let us consider a spherically symmetric nucleus with isotropic and homogeneous distribution of nuclear matter $\rho(r) = \rho_0 \theta(r_A - r)$, having radius r_A ($(4\pi/3)r_A^3 \rho_0 = A$). For this model of nucleus in the Glauber approximation [49], i.e. in the case when in the interaction point the virtual photon produces a fast hadron h (in this case $\tau=0$), the cross section of interaction of which with the nucleons in nucleus is equal to σ_h , for the value of nuclear transparency $R = \sigma(\gamma^V A \rightarrow hX) / A\sigma(\gamma^V N \rightarrow hX)$ we have:

$$R = R(\xi) = \frac{3}{2\xi} \left\{ 1 - \frac{2}{\xi^2} [1 - (1+\xi)\exp(-\xi)] \right\} \quad (A.1)$$

where $\xi = 2r_A \rho_0 \sigma_h = (3/2)(A\sigma_h/\pi r_A^2) \sim A^{1/3} \sigma_h$. The limit values of the function $R(\xi)$ plotted in Fig.11 are obvious: $R(0)=1$ and $R(\xi) \approx 3/2\xi = \pi r_A^2 / A\sigma_h \sim 1/A^{1/3} \sigma_h$, if $\xi \rightarrow \infty$. The expression (A.1) shows that the only parameter characterizing the yield of hadrons h from nucleus A is the value of $\xi \sim A^{1/3} \sigma_h$. Hence, the experiments with registration of the same hadron h on different nuclei A and A_1 , or with registration of different hadrons h and h_1 on the same nucleus A are completely identical from the point of view of the analysis of the model considered at $\sigma_h A_1^{1/3} = \sigma_{h_1} A^{1/3}$.

Let us pass to considering the case when $\tau > 0$ and $\sigma_q < \sigma_h$. For this we shall start considering the case when the law of changing of the cross section from σ_q to σ_h on the time/distance variable t looks like a stair.

$$\sigma_1(t) = \sigma_q \theta(t) + (\sigma_h - \sigma_q) \theta(t - \tau). \quad (A.2)$$

The starting point for the time is considered the moment of interaction of γ^V with nuclear matter, though, actually, this

is not a point, as mentioned in the Introduction, but some space-time region having dimensions of the order of τ_p , but at high values of Q^2 its dimensions are much less than $\tau_F \gg \tau_p$.

In the frameworks of such a model, for the value of nuclear transparency R we have:

$$R = R_1(\xi; \alpha, \beta) = \frac{3}{2\xi} \{ (1-\beta^2) [e^{-\alpha\xi} + (1-e^{-\alpha\xi})/\alpha] - \frac{2e^{(1-\alpha)\beta\xi}}{\xi^2} \times \quad (A.3)$$

$$\times [(1+\beta\xi)e^{-\beta\xi} - (1+\xi)e^{-\xi}] + \frac{\beta^2}{\alpha} [1 - \frac{2}{(\alpha\xi)^2} (1 - (1+\alpha\xi)e^{-\alpha\xi})],$$

where, as in (A.1), $\xi = d_A \rho_0 \sigma_h$ ($d_A = 2r_A$ is diameter of the nucleus), $\alpha = \sigma_q / \sigma_h$ and $\beta = \tau / d_A$. The limit values for $R_1(\xi; \alpha, \beta)$ are the following:

$$R_1(\xi; 0, \beta) = \frac{3}{2\xi} \{ (1-\beta^2)(1+\beta\xi) + \frac{2\xi}{3} \beta^2 - \quad (A.4a)$$

$$- \frac{2}{\xi^2} [(1+\beta\xi) - (1+\xi)e^{-(1-\beta)\xi}] \}$$

$$R_1(\xi; 0, 0) = R(\xi) \quad (A.4b)$$

$$R_1(\xi; 0, 1) = 1 \quad (A.4c)$$

$$R_1(\xi; 1, \beta) = R(\xi) - \text{does not depend on } \beta \quad (A.4d)$$

$$R_1(\xi; \alpha, 0) = R(\xi) - \text{does not depend on } \alpha \quad (A.4e)$$

$$R_1(\xi; \alpha, 1) = R(\alpha\xi) \quad (A.4f)$$

The dependence of R for the ^{64}Cu nucleus on τ at different values of ξ and α ($\alpha=0$ and $\alpha=0.2$) is shown in Fig.12, where the results of Monte-Carlo simulation are also given on the basis of the expression (1) and for the Wood-Saxon nuclear density

distribution $\rho(r) = \rho_0 / (1 + \exp((r - r_A)/a))$, where $a = 0.54$ and $r_A = (0.978 + 0.0206A^{1/3})A^{1/3}$ [2]. For example, for the ^{64}Cu nucleus ($r_A = 4.24F$ and $\rho_0 = 0.17F^{-3}$) at $\xi_{\text{eff}} = 2.3$ (when $r_A^{\text{eff}} = 5.15F$ and $\rho_0 = 0.11F^{-3}$) the results of calculation by (A.3) practically for all values of σ_q do not sufficiently differ from the results of the Monte-Carlo simulation by the Wood-Saxon nuclear density distribution obtained on the basis of the expression (1).

In numerical calculations carried out in the frameworks of the models $\sigma(t) \sim t$ and $\sigma(t) \sim t^2$, there were correspondingly used the following expressions:

$$\sigma_2(t) = \sigma_h - (\sigma_h - \sigma_q) \exp(-t/\tau), \quad (\text{A.5a})$$

$$\sigma_3(t) = \sigma_h - (\sigma_h - \sigma_q) \exp(-t^2/\tau^2). \quad (\text{A.5b})$$

The following expressions were considered in Ref. [5]:

$$\sigma_4(t) = \left(\sigma_q + \frac{\sigma_h - \sigma_q}{\tau} t \right) \theta(\tau - t) + \sigma_h \theta(t - \tau), \quad (\text{A.6a})$$

$$\sigma_5(t) = \left(\sigma_q + \frac{\sigma_h - \sigma_q}{\tau^2} t^2 \right) \theta(\tau - t) + \sigma_h \theta(t - \tau), \quad (\text{A.6b})$$

which correspond to $\sigma_2(t)$ and $\sigma_3(t)$, respectively, at $t/\tau \ll 1$ and $t \gg \tau$.

The option $\sigma_4(t)$ and also $\sigma_2(t)$ at $t \ll \tau$ correspond to the predictions of perturbative QCD and they have $\sim t$ -like behaviour at $t \ll \tau$. The option $\sigma_5(t)$ and also $\sigma_3(t)$ at $t \ll \tau$ have $\sim t^2$ -like behaviour in correspondence with the predictions of the colour dipole model. The dependences $\sigma_2(t)$ and $\sigma_3(t)$ differ from $\sigma_4(t)$ and $\sigma_5(t)$ in the region $t \sim \tau$ only, where in contrast with $\sigma_4(t)$ and $\sigma_5(t)$, they provide a smooth transition of the cross section from the $t \ll \tau$ region (perturbative QCD range) to $t \geq \tau$ region (non-perturbative QCD range).

The case analogous to $\sigma_1(t)$ is also considered in the literature, but with an exponentially distributed quark-to-hadron transition point $P_{q \rightarrow h}(t) = \exp(-t/\tau)/\tau$ [53]. It is not difficult to notice that such a model is completely equivalent to the one with the following $\sigma_6(t)$ dependence:

$$\sigma_6(t) = \frac{\sigma_h - (\sigma_h - \sigma_q)(1 + \tau \rho_0 \sigma_q) \exp(\rho_0 t (\sigma_h - \sigma_\tau))}{1 - (\sigma_h - \sigma_q) \tau \rho_0 \exp(\rho_0 t (\sigma_h - \sigma_\tau))}, \quad (\text{A.7})$$

where $\sigma_\tau = \sigma_q + 1/\tau \rho_0$. The peculiarity and distinction of such a dependence is that it contains nuclear characteristics, namely, nucleus density ρ_0 . The dependence of $\sigma_6(t)$ on the time variable t has the following unexpected behaviour in the limit $t \rightarrow \infty$, that is:

$$\sigma_6(t) \rightarrow \sigma_h \quad \text{if} \quad 0 \leq \tau \leq \tau_c, \quad (\text{A.8a})$$

$$\sigma_6(t) \rightarrow \sigma_\tau = \sigma_q + 1/\rho_0 \tau < \sigma_h \quad \text{if} \quad \tau > \tau_c, \quad (\text{A.8b})$$

where $\tau_c = 1/\rho_0(\sigma_h - \sigma_q)$. However, at $t/\tau \ll 1$ the expression for $\sigma_6(t)$ has an asymptotics

$$\sigma_6(t) \approx \sigma_q + \frac{\sigma_h - \sigma_q}{\tau} t \quad (\text{A.9})$$

and is consistent with the expressions for $\sigma_2(t)$ and $\sigma_4(t)$ at $t/\tau \ll 1$.

In our notations, in case of $\sigma_6(t)$ dependence, for the nuclear transparency R we have [53]:

$$R = R_6(\xi; \alpha, \beta) = \frac{R(\xi) - (1-\alpha)\beta\xi R(\alpha\xi + 1/\beta)}{1 - (1-\alpha)\beta\xi} \quad (\text{A.10})$$

and if $1 - (1-\alpha)\beta\xi = 0$, we have

$$R_6(\xi; \alpha, \beta) = R(\xi) - R'(\xi)/\beta, \quad (\text{A.11})$$

where $R'(\xi) = dR(\xi)/d\xi = (3/\xi)[(1 - e^{-\xi})/\xi - R(\xi)]$ and $R'(0) = -3/8$.

The expressions (A.10) and (A.11) are always positive, because the values of $R(\xi)$ are monotonously decreasing functions of ξ . The limit values for $R_\delta(\xi; \alpha, \beta)$ are the following:

$$R_\delta(\xi; 0, \beta) = \frac{R(\xi) - \beta \xi R(1/\beta)}{1 - \beta \xi} \quad (\text{A.12a})$$

$$R_\delta(\xi; 0, 0) = R(\xi) \quad (\text{A.12b})$$

$$R_\delta(\xi; 0, \infty) = 1 \quad (\text{A.12c})$$

$$R_\delta(\xi; 1, \beta) = R(\xi) - \text{does not depend on } \beta \quad (\text{A.12d})$$

$$R_\delta(\xi; \alpha, 0) = R(\xi) - \text{does not depend on } \alpha \quad (\text{A.12e})$$

$$R_\delta(\xi; \alpha, \infty) = R(\alpha \xi) . \quad (\text{A.12f})$$

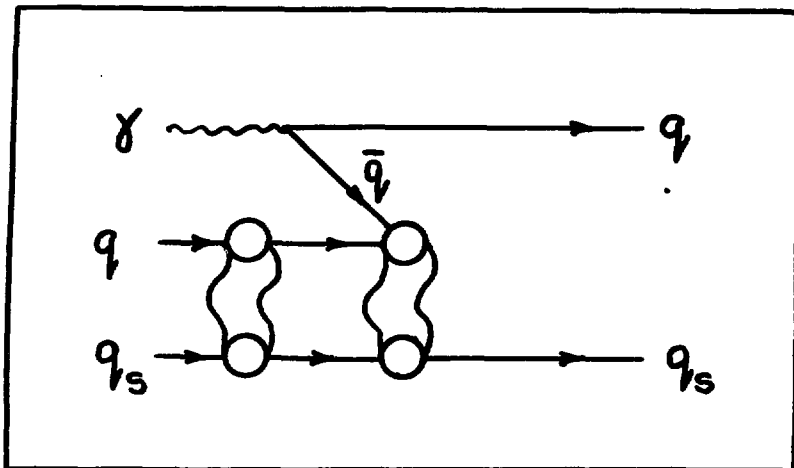


Fig.1a

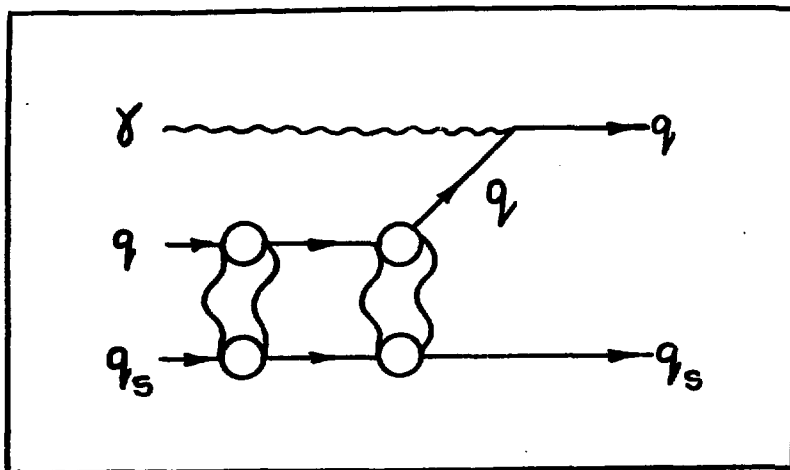


Fig.1b

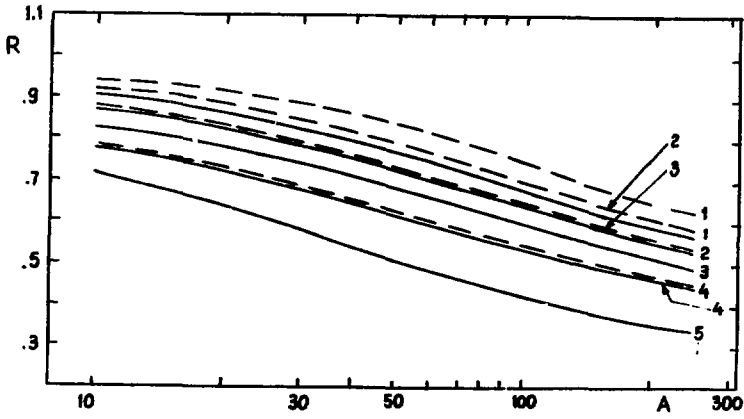


Fig.2a

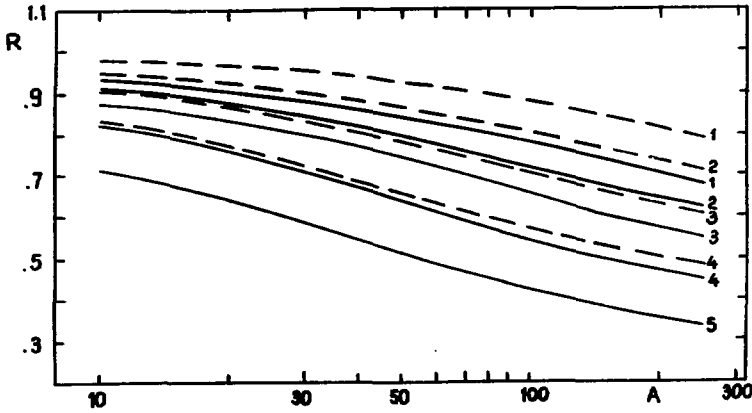
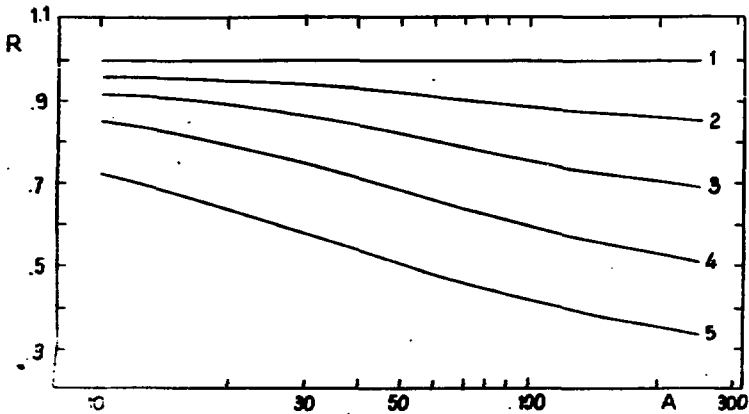


Fig.2b



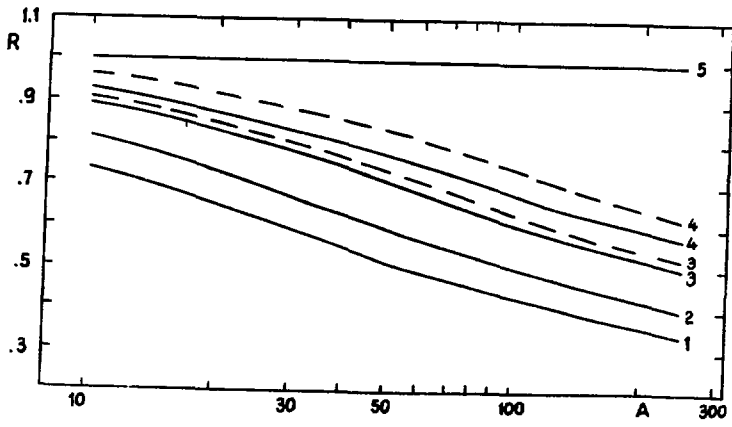


Fig. 3a

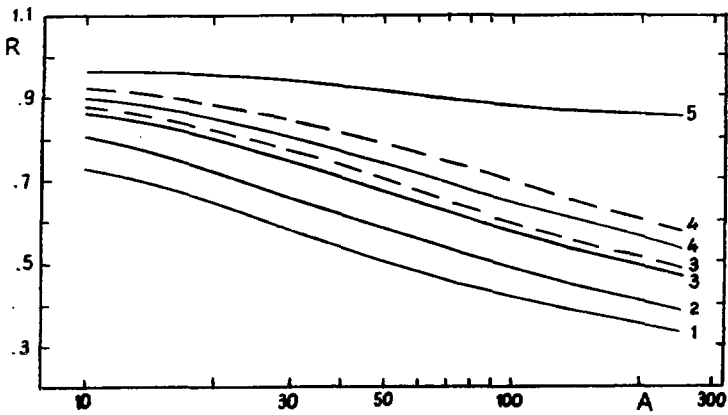


Fig. 3b

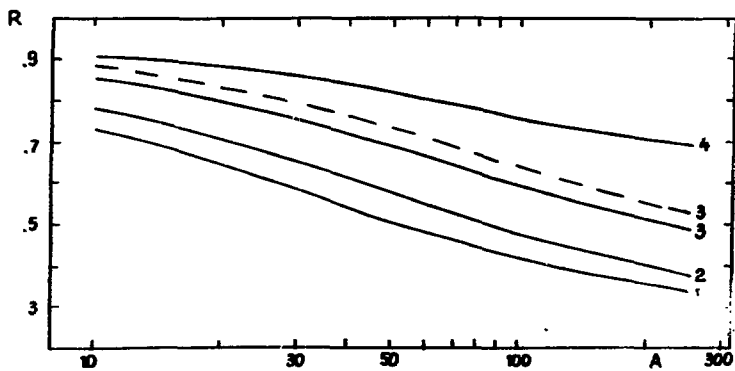


Fig. 3c

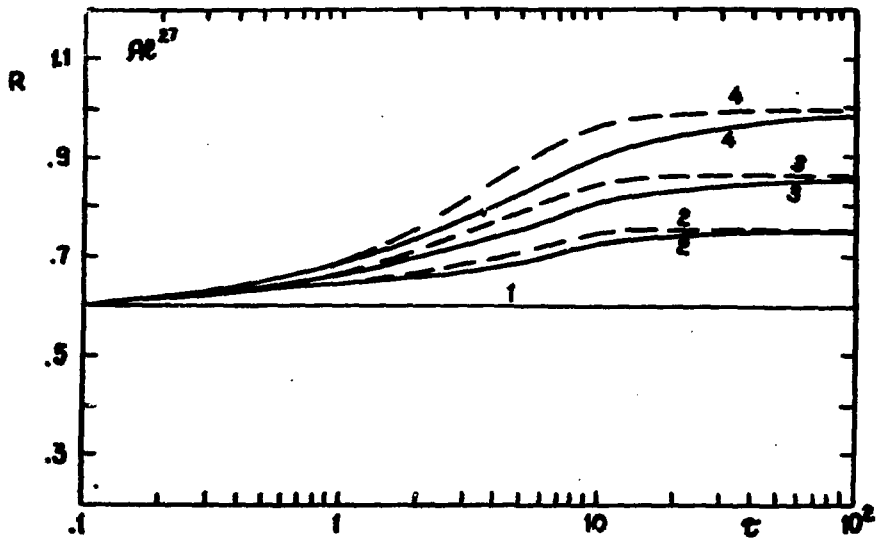


Fig.4a

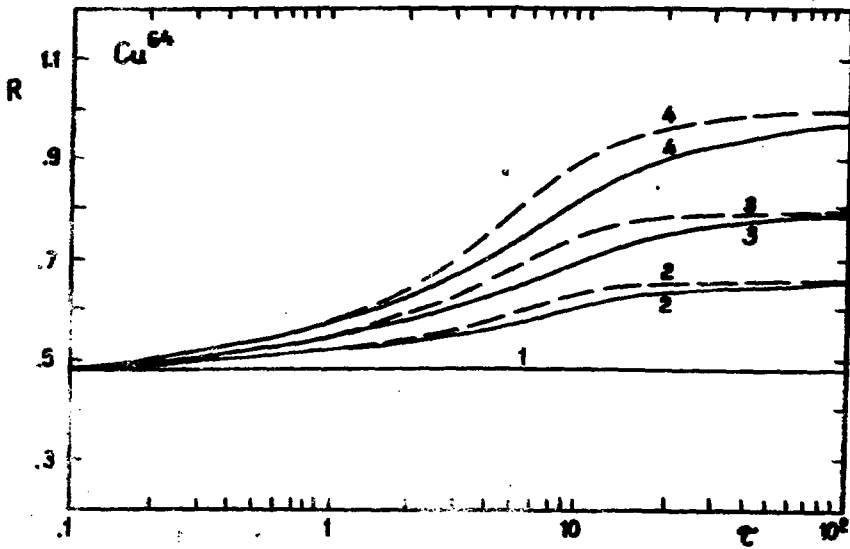


Fig.4b

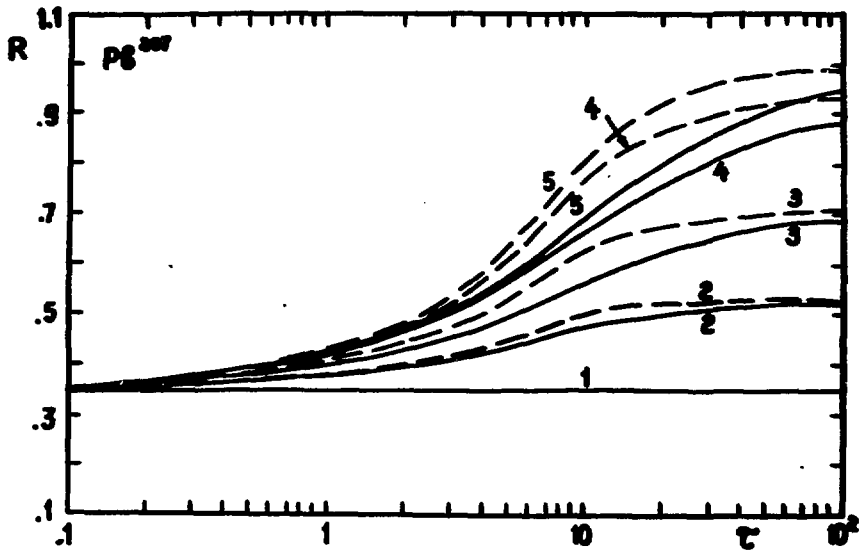


Fig. 4c

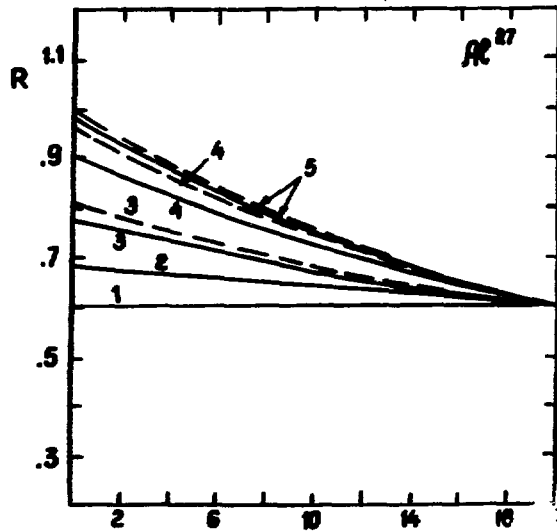


Fig. 5a

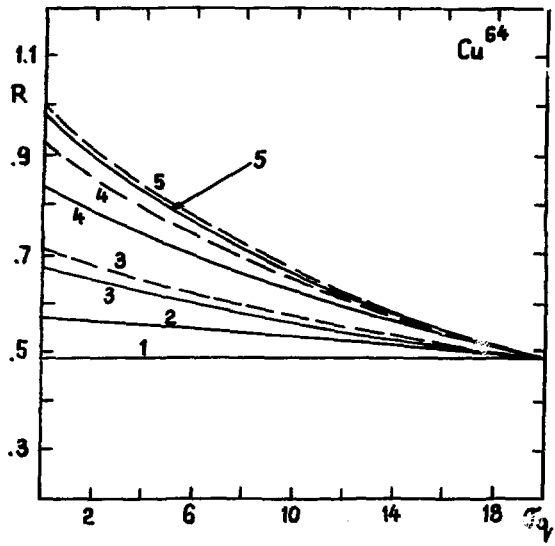


Fig.5b

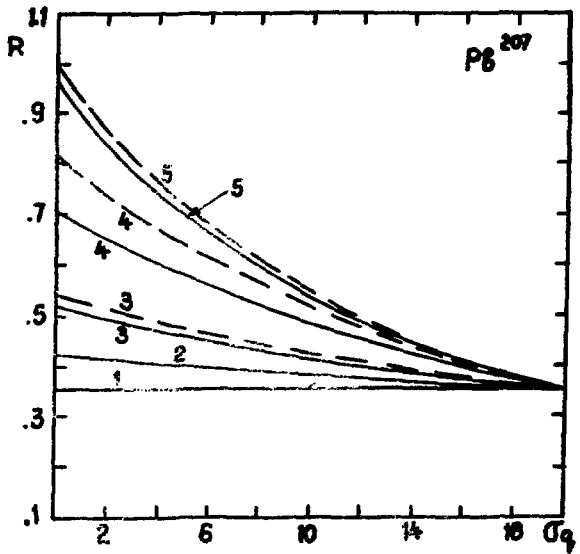


Fig.5c

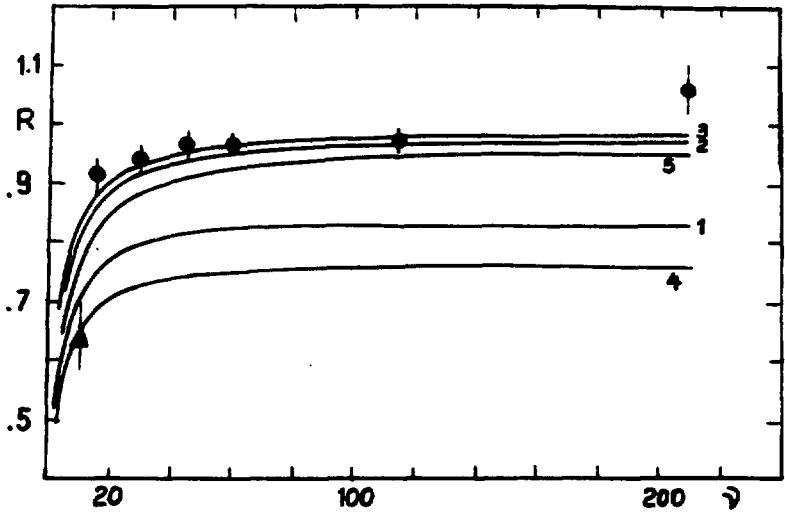


Fig.6

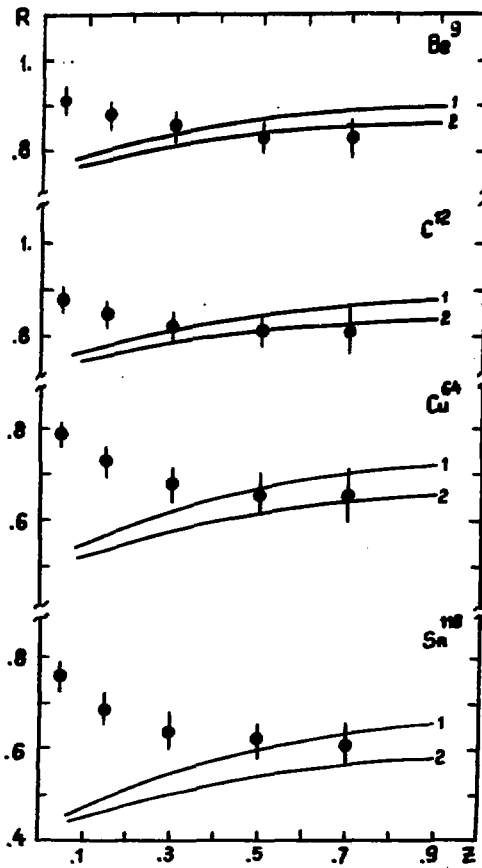


Fig./a

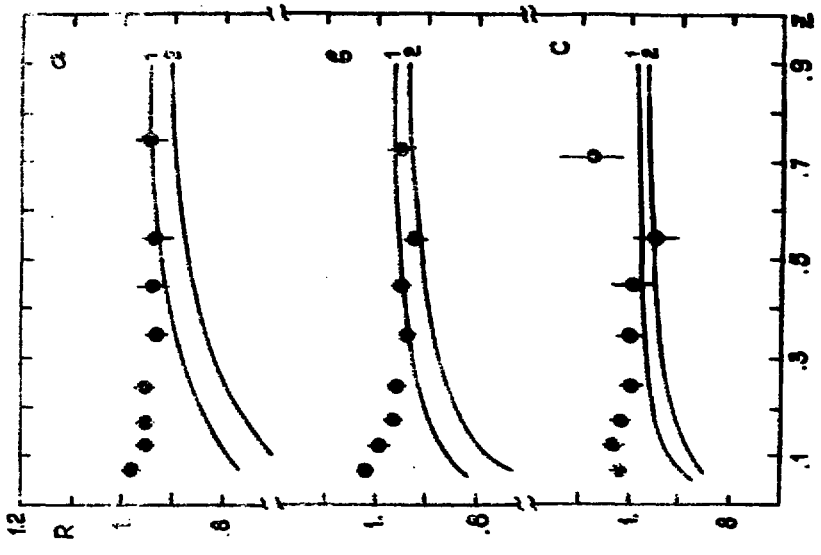


Fig. 7b

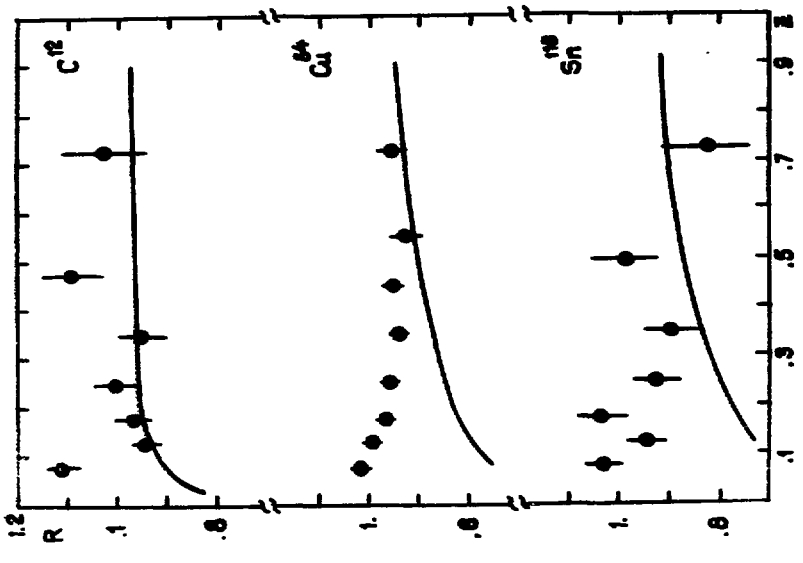


Fig. 7c

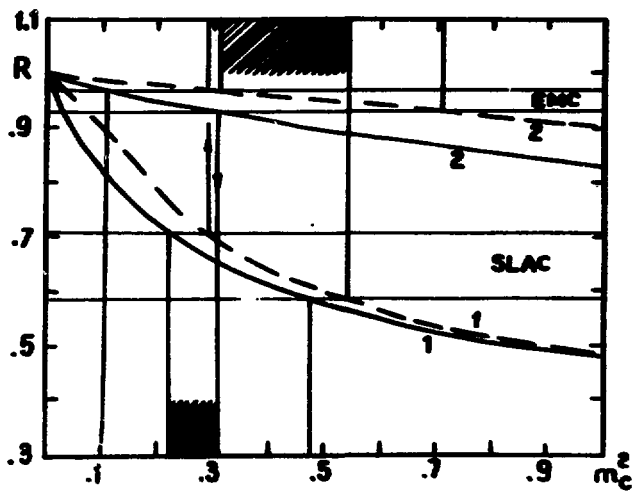


Fig.8

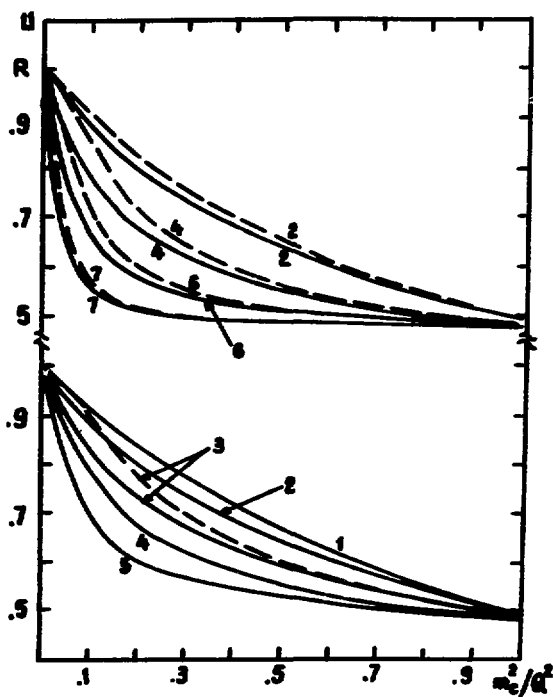


Fig.9a

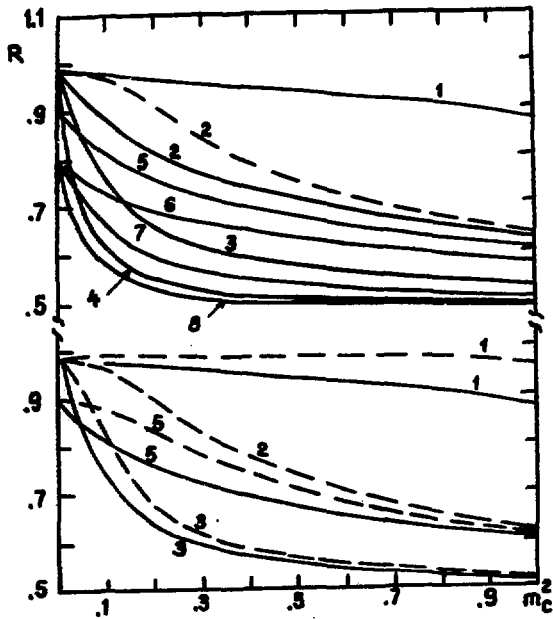


Fig.9b

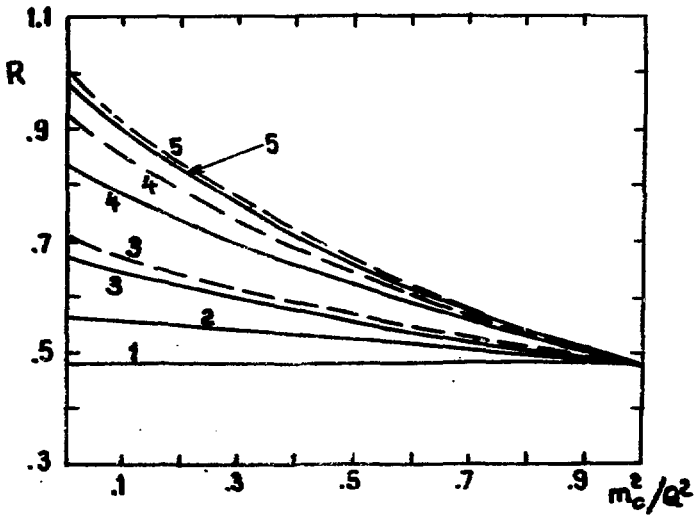


Fig.9c

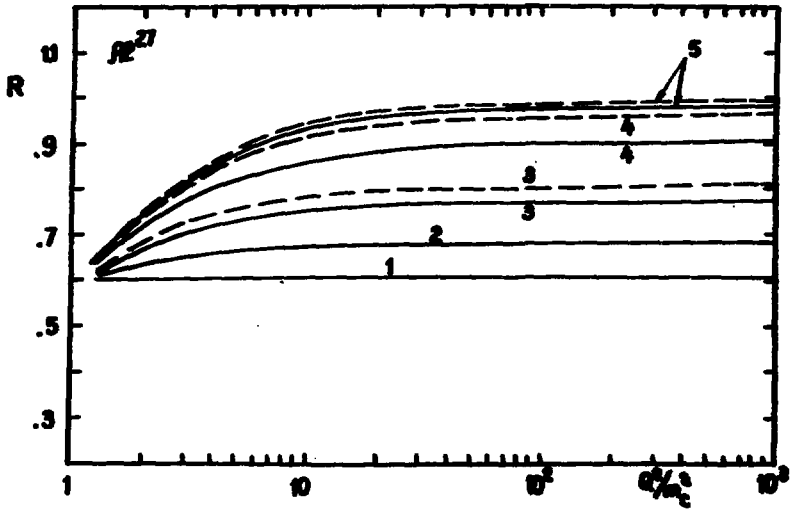


Fig.10a

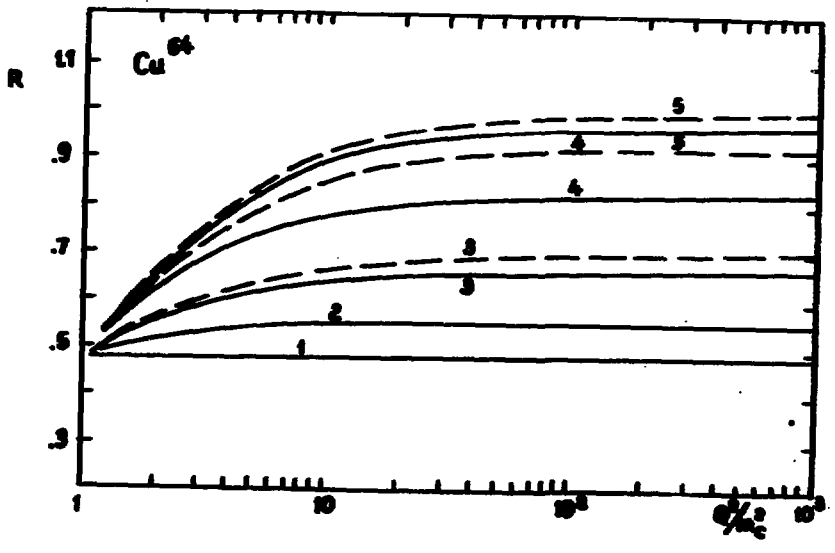


Fig.10b

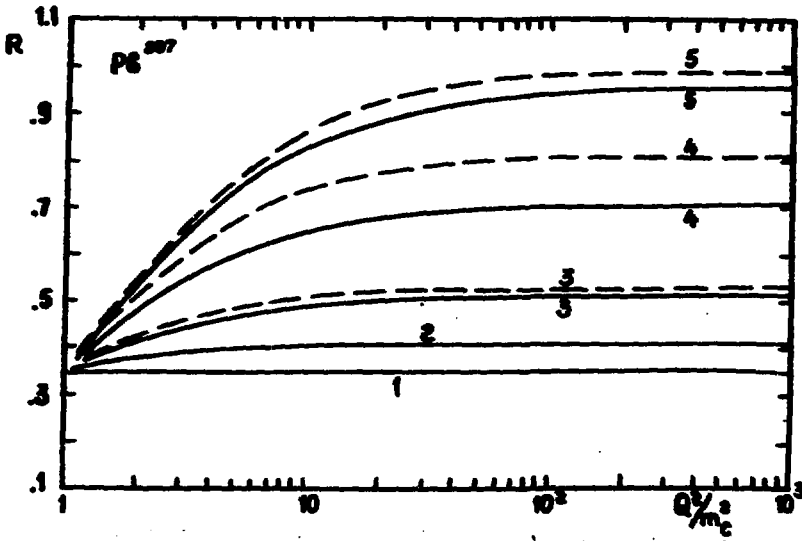


Fig. 10c

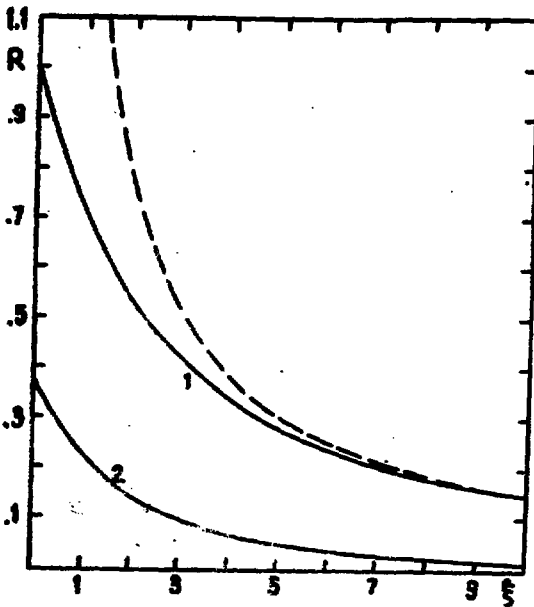


Fig. 11

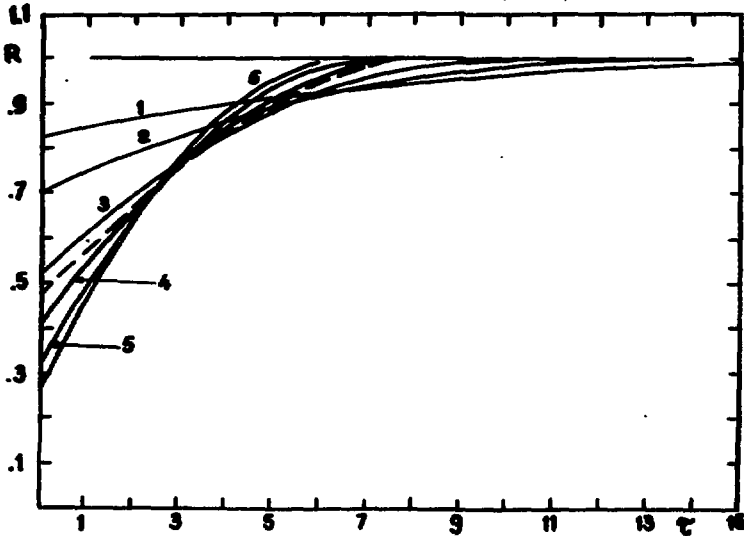


Fig. 12a

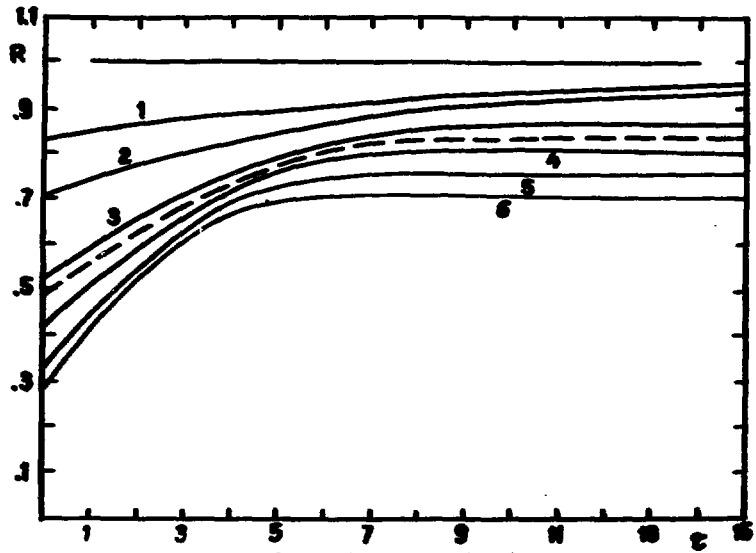


Fig. 12b

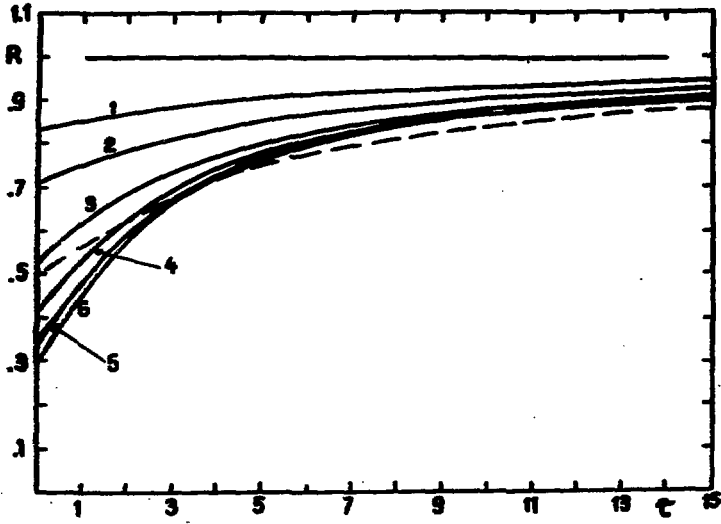


Fig.12c

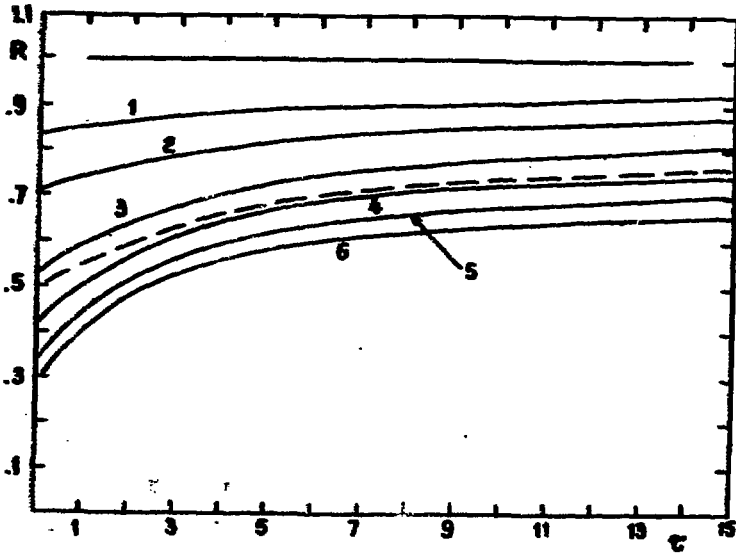


Fig.12d

Figure Captions

- Fig.1 The interaction mechanism of photon with quark of the nucleon of nucleus in the rest frame of nucleus (a), and in the Breit frame (b).
- Fig.2 Dependence of nuclear transparency R on atomic number A at $\tau=5F$ (a), $\tau=10F$ (b), $\tau \rightarrow \infty$ (c). Curves: 1 - $\sigma_q=0$; 2 - $\sigma_q=2\text{mb}$; 3 - $\sigma_q=5\text{mb}$; 4 - $\sigma_q=10\text{mb}$; 5 - $\sigma_q=\sigma_h=20\text{mb}$. Solid curves are the model $\alpha(t) \cdot t$, dashed curves are $\alpha(t) \cdot t^2$.
- Fig.3 Dependence of nuclear transparency R on atomic number A at $\sigma_q=0$ (a), $\sigma_q=2\text{mb}$ (b), $\sigma_q=5\text{mb}$ (c). Curves: 1 - $\tau=0$; 2 - $\tau=1F$; 3 - $\tau=3F$ (a and b) and $\tau=5F$ (c); 4 - $\tau=5F$ (a,b) and $\tau \rightarrow \infty$ (c); 5 - $\tau \rightarrow \infty$ (a,b). Solid curves are the model $\alpha(t) \cdot t$, dashed curves are $\alpha(t) \cdot t^2$.
- Fig.4 Dependence of nuclear transparency R on $\tau(F)$ for ^{27}Al (a), ^{64}Cu (b) and ^{207}Pb (c) nuclei. Curves: 1 - $\sigma_q=\sigma_h=20\text{mb}$; 2 - $\sigma_q=10\text{mb}$; 3 - $\sigma_q=5\text{mb}$; 4 - $\sigma_q=0$ (a,b) and $\sigma_q=1\text{mb}$ (c); 5 - $\sigma_q=0$ (c). Solid curves are the model $\alpha(t) \cdot t$, dashed curves are $\alpha(t) \cdot t^2$.
- Fig.5 Dependence of R on $\sigma_q(\text{mb})$ for ^{27}Al (a), ^{64}Cu (b) and ^{207}Pb (c) nuclei. Curves: 1 - $\tau=0$; 2 - $\tau=1F$; 3 - $\tau=3F$; 4 - $\tau=10F$; 5 - $\tau=100F$. Solid curves are the model $\alpha(t) \cdot t$, dashed curves are $\alpha(t) \cdot t^2$.
- Fig.6 Dependence of nuclear transparency R on photon energy $\nu(\text{GeV})$ for the ^{64}Cu nucleus. Experimental points: Δ - SLAC [44]; \bullet - EMC CERN [45]. Curves are calculated for the model $\alpha(t) \cdot t$ ($z=1$) with two values of the parameter $m_C^2=0.2\text{GeV}^2$ (curves: 1 - $Q^2=1\text{GeV}^2$; 2 - $Q^2=10\text{GeV}^2$; 3 - $Q^2 \rightarrow \infty$) and $m_C^2=0.3\text{GeV}^2$ (curves: 4 - $Q^2=1\text{GeV}^2$; 5 - $Q^2=10\text{GeV}^2$).

Fig.7 Dependence of R on z for the model $\alpha(t)\sim t$. a - the SLAC data [44] for the ${}^9\text{Be}$, ${}^{12}\text{C}$, ${}^{64}\text{Cu}$ and ${}^{118}\text{Sn}$ nuclei. Curves are calculated at mean values of $\nu=10\text{GeV}$ and $Q^2=1\text{GeV}^2$ (curve 1 - $m_C^2=0.2\text{GeV}^2$, 2 - $m_C^2=0.3\text{GeV}^2$); b - the EMC CERN data [45] for the ${}^{64}\text{Cu}$ nucleus with different mean values of photon energy $\bar{\nu}=35\text{GeV}$ (a), $\bar{\nu}=60\text{GeV}$ (b), $\bar{\nu}=145\text{GeV}$ (c). Curves are calculated at the corresponding values of photon energy ν and at $Q^2=10\text{GeV}^2$ (curve 1 - $m_C^2=0.1\text{GeV}^2$, 2 - $m_C^2=0.2\text{GeV}^2$); c - the EMC CERN points [45] for the ${}^{12}\text{C}$, ${}^{64}\text{Cu}$ and ${}^{118}\text{Sn}$ nuclei at $\bar{\nu}=60\text{GeV}$. Curves: $\nu=60\text{GeV}$, $Q^2=15\text{GeV}^2$ and $m_C^2=0.2\text{GeV}^2$.

Fig.8 Within the range of $0.22\text{GeV}^2 \leq m_C^2 \leq 0.31\text{GeV}^2$ in the frameworks of the model $\alpha(t)\sim t$ and $0.31\text{GeV}^2 \leq m_C^2 \leq 0.54\text{GeV}^2$ in the frameworks of the model $\alpha(t)\sim t^2$ the experimental data obtained in SLAC [44] and EMC CERN [45] can be self-consistently described on the basis of the expressions (1)-(3). Curves: 1 - $\nu=10\text{GeV}$, $Q^2=1\text{GeV}^2$; 2 - $\nu=100\text{GeV}$, $Q^2=10\text{GeV}^2$. Solid curves 1 and 2 are the model $\alpha(t)\sim t$; dashed curves are the model $\alpha(t)\sim t^2$.

Fig.9 Dependence of nuclear transparency R of ${}^{64}\text{Cu}$ nucleus on m_C^2/Q^2 (a): Curves: 1 - $x_B=0.001$; 2 - $x_B=0.01$; 3 - $x_B=0.05$; 4 - $x_B=0.1$; 5 - $x_B=0.2$; 6 - $x_B=0.3$; 7 - $x_B=1$, on m_C^2 (b): curves: (1-4) - $\sigma_q=0$ (1 - $z\nu=100\text{GeV}$, 2 - $z\nu=10\text{GeV}$, 3 - $z\nu=3\text{GeV}$ and 4 - $z\nu=1\text{GeV}$); 5 - $\sigma_q=2\text{mb}$ and $z\nu=10\text{GeV}$; (6-8) - $\sigma_q=5\text{mb}$ (6 - $z\nu=10\text{GeV}$, 7 - $z\nu=3\text{GeV}$ and 8 - $z\nu=1\text{GeV}$), on m_C^2/Q^2 (c): curves: 1 - $\tau=0$; 2 - $\tau=1\text{F}$; 3 - $\tau=3\text{F}$; 4 - $\tau=10\text{F}$; 5 - $\tau=100\text{F}$. Solid curves are the model $\alpha(t)\sim t$, dashed curves are $\alpha(t)\sim t^2$.

Fig.10 Dependence of nuclear transparency R for the ^{27}Al (a), ^{64}Cu (b) and ^{207}Pb (c) nuclei on the variable Q^2/m_c^2 . Curves: 1 - $\tau=0$; 2 - $\tau=1F$; 3 - $\tau=3F$; 4 - $\tau=10F$; 5 - $\tau=100F$. Solid curves are the model $\alpha(t)-t$, dashed curves are $\alpha(t)-t^2$.

Fig.11 The functions $R(\xi)$ (curve 1) and $|R'(\xi)|$ (curve 2). Dashed curve shows the dependence $3/2\xi$.

Fig.12 Dependence of R on $\tau(F)$ for the ^{64}Cu nucleus obtained on the basis of the expression (A.3) ($a - \sigma_q=0$, $b - \sigma_q=4mb$) and (A.10) ($c - \sigma_q=0$, $d - \sigma_q=4mb$) at different values of ξ . Curves: 1 - $\xi=0.5$; 2 - $\xi=1$; 3 - $\xi=2$; 4 - $\xi=3$; 5 - $\xi=4$; 6 - $\xi=5$. Dashed curves - calculations with the Wood-Saxon nuclear density.

References

1. Bialas A. Acta Phys. Pol.B, 1980, vol.11, No.6, p.475-480.
2. Bialas A., Chmaj T. Phys.Lett.B, 1983, vol.133, No.3/4 p.241-244.
3. Nikolaev N.N. Usp. Fiz. Nauk, 1981, vol.134, No.3, p.369-430.
4. Brodsky S.J., Mueller A.H. Phys.Lett.B, 1988, vol.206, No.4, p.685-690.
5. Farrar G.R., Liu H., Frankfurt L.L., Strikman M.I. Phys. Rev.Lett., 1988, vol.61, No.6, p.686-689.
6. Chmaj T. Acta Phys. Pol.B, 1987, vol.18, No.12, p.1131-1140.
7. Bialas A., Gyulassy M. Nucl.Phys.B, 1987, vol.291, No.4, p.793-812.
8. Bialas A., Czyzewski J. Phys.Lett.B, 1989, vol.222, No.1, p.132-134.
9. Gyulassy M., Plumer M. Nucl.Phys.B, 1990, vol.346, No.1, p.1-16.
10. Saxon D.H. Preprint RAL-86-057, Rutherford Appleton Laboratory, Chilton, 1986.
11. Reya E. Phys.Rep.C, 1981, vol.69, No.3, p.195-333.
12. Altarelli G. Phys.Rep.C, 1982, vol.81, No.1, p.1-129.
13. Collins P.D.B., Martin A.D. Rep.Prog.Phys., 1982, vol.45, No.4, p.335-426.
14. Fialkowski K., Kittel W. Rep.Prog.Phys., 1983, vol.46, No.11, p.1283-1392.
15. Fild R.D., Feynman R.P. Nucl.Phys.B, 1978, vol.136, No.1, p.1-76.
16. Ilgenfritz E.M., Kripfganz J., Schiller A. Acta Phys.Pol. B, 1978, vol.9, No.10, p.881-900.

17. Sukhatme U.P., Lassila K.E., Orava R. Phys.Rev.D, 1982, vol.25, No.11, p.2975-2987.
18. Bartl A., Fraas H., Majerotto W. Phys.Rev.D, 1982, vol.26, No.5, p.1061-1075.
19. Minakata H. Phys.Rev.D, 1979, vol.20, No.7, p.1656-1665.
20. Kaidalov A.B. Yad. Fiz., 1987, vol.45, No.5, p.1452-1461.
21. Marchesini G., Webber B.R. Nucl.Phys.B, 1984, vol.238, No.1, p.1-29.
22. Webber B.R. Nucl.Phys.B, 1984, vol.238, No.3, p.492-528.
23. Andersson B., Gustafson G., Ingelman G., Sjostrand T. Phys.Rep.C, 1983, vol.97, No.2/3, p.31-145.
24. Chang V., Hwa R.C. Phys.Rev.Lett., 1980, vol.44, No.7, p.439-442.
25. Chang V., Hwa R.C. Phys.Rev.D, 1981, vol.23, No.3, p.728-741.
26. Jones L.M., Lassila K.E., Sukhatme U., Willen D. Phys.Rev. D, 1981, vol.23, No.3, p.717-727.
27. Hwa R.C. Hadron structure and the hadronization of quarks. Proc. of the 1980 Guangzhou Conf. on Theor. Particle Phys., vol.1, New York: Van Nostrand 1980.
28. Eilam G., Zahir M.S. Phys.Rev.D, 1982, vol.26, No.11, p.2991-3001.
29. Badalyan R.G. Yad. Fiz., 1988, vol.47, No.1, p.220-229.
30. Badalyan R.G. Yad. Fiz., 1989, vol.50, No.4(10), p.1120-1131.
31. Das K.P., Hwa R.C. Phys.Lett.B, 1977, vol.68, No.5, p.459-462.
32. Hwa R.C. Phys.Rev.D, 1980, vol.22, No.7, p.1593-1608.
33. Takasugi E., Tata X., Chiu C.B., Kaul R. Phys.Rev.D, 1979, vol.20, No.1, p.211-220.

34. Badalyan R.G., Gulkanyan H.G. *Yad. Fiz.*, 1985, vol.41, No.6, p.1611-1621.
35. Feynman R.P. *Photon Hadron Interactions*, W.A. Benjamin, New York, 1972.
36. Gribov V.N. *Proc. VIII Winter School LINP, Leningrad*, 1973, p.5-36.
37. Bjorken J.D. *Hadron final states in deep inelastic processes. in: Current induced reactions. Proc. Int. Summer Institute on Theor. Particle Phys.*, p.93-158, Hamburg, 1975.
38. Bauer T.H., Spital R.D., Yennie D.R., Pipkin F.M. *Rev.Mod.Phys.*, 1978, vol.50, No.2, p.261-436.
39. Azimov Ya.I., Dokshitzer Yu.L., Khoze V.A. *Proc. XVII Winter School LINP, Leningrad*, 1982, p.162-225.
40. Gribov L.V., Dokshitzer Yu.L., Troyan S.I., Khoze V.A. *Proc. XXII Winter School LINP, Leningrad*, 1987, p.61-103.
41. Franz J. et al. *Z.Phys.C*, 1981, vol.10, No.2, p.105-116.
42. Ashman J. et al. *Phys.Lett.B*, 1988, vol.202, No.4, p.603-610.
43. Amodeo M. et al. *Phys.Lett.B*, 1988, vol.211, No.4, p.493-499.
44. Osborne L.S. et al. *Phys.Rev.Lett.*, 1978, vol.40, No.25, p.1624-1627.
45. Arvidson A. et al. *Nucl.Phys.B*, 1984, vol.246, No.3, p.381-407.
46. Baranov D.S. et al. *Yad. Fiz.*, 1984, vol.40, No.6(12), p.1454-1459.
47. Badalyan R.G. et al. *Preprint YERPHI-1304(90)-90, Yerevan*, 1990.
48. Arnold R.G. et al. *Preprint SLAC-377*, 1990.
49. Glauber R. *Usp. Fiz. Nauk*, 1971, vol.103, No.4, p.641-673.

50. Badalyan N.N., Badalyan R.G. Z.Phys.C, 1990, vol.48, No.4, p.587-594.
51. Berger E.L., Brodsky S.J. Phys.Rev.Lett., 1979, vol.42, No.15, p.940-944.
52. Berger E.L. Phys.Lett.B, 1980, vol.89, No.2, p.241-245.
53. Gevorkyan S.R., Gulkanyan H.R. Yad. Fiz., 1982, vol.36, No.6(12), p.1504-1509.

The manuscript was received December 7, 1990

Р. Г. БАДАЛЯН

МЕХАНИЗМ ФОРМИРОВАНИЯ БЫСТРЫХ АДРОНОВ

В ПРОЦЕССАХ ЛЕПТОРОЖДЕНИЯ В ЯДРАХ

(на английском языке, перевод Г. А. Папяна)

Редактор Л. П. Мукаян

Технический редактор А. С. Абрамян

Подписано в печать 23/XII-90
Офсетная печать. Уч. изд. л. 2,0
Зак. тип. 363

Формат 60×84×16
Тираж 299 экз. Ц. 30к.
Индекс 3649

Отпечатано в Ереванском физическом институте
Ереван-36, ул. Братьев Алиханян 2.

**The address for requests:
Information Department
Yerevan Physics Institute
Alikhanian Brothers 2,
Yerevan, 375036
Armenia, USSR**

ИНДЕКС 3649



ЕРЕВАНСКИЙ ФИЗИЧЕСКИЙ ИНСТИТУТ